nature cell biology

A mechanism for chromosome segregation sensing by the NoCut checkpoint

Manuel Mendoza[1,3], Caren Norden[1,4], Kathrin Durrer[1], Harald Rauter[1], Frank Uhlmann[2] and Yves Barral[1,5]

In *Saccharomyces cerevisiae*[1] and HeLa cells[2], the NoCut checkpoint, which involves the chromosome passenger kinase Aurora B, delays the completion of cytokinesis in response to anaphase defects. However, how NoCut monitors anaphase progression has not been clear. Here, we show that retention of chromatin in the plane of cleavage is sufficient to trigger NoCut, provided that Aurora/Ipl1 localizes properly to the spindle midzone, and that the ADA histone acetyltransferase complex is intact. Furthermore, forcing Aurora onto chromatin was sufficient to activate NoCut independently of anaphase defects. These findings provide the first evidence that NoCut is triggered by the interaction of acetylated chromatin with the passenger complex at the spindle midzone.

During mitosis, the spindle assembly checkpoint delays the onset of anaphase until all chromosomes are properly attached to spindle microtubules[3,4]. Subsequently, sister-chromatids separate and the cleavage furrow starts to pinch the cell[5,6]. However, cell cleavage, or abscission, does not occur until all chromatids are retracted from the cleavage plane[1,2]. How cells coordinate abscission and chromosome segregation is poorly understood.

In *S. cerevisiae*, inactivation of spindle midzone components, such as Ase1 or Ndc10, causes premature spindle breakage and compromises chromosome segregation. In these cells, furrow ingression proceeds properly but abscission is delayed by the NoCut pathway, preventing damage of stranded chromosomes by cytokinesis[1]. The chromosome passenger complex (CPC), consisting of the Aurora kinase Ipl1 and its regulator INCENP/Sli15 (refs 7, 8), acts at the top of the NoCut pathway. It conveys the NoCut signal by targeting the NoCut effectors Boi1 and Boi2, two anillin-like proteins, to the site of cleavage at the bud neck[1]. CPC-dependent transfer of Boi1 and Boi2 to the bud neck occurs in every anaphase, but is relieved at the onset of cytokinesis, after proper completion of anaphase. In cells with spindle defects, Boi1 and Boi2 remain at the bud neck and abscission is delayed. However, the exact event triggering the NoCut response is unknown. Interestingly, NoCut function is conserved in HeLa cells, where human Aurora B delays abscission in cells with chromosome bridges[2]. To investigate how Aurora kinase monitors completion of anaphase in *S. cerevisiae*, we first assessed whether NoCut responds to lagging chromatin in the absence of spindle defects.

The topoisomerase II (Top2) mutant *top2-4* fails to decatenate sister chromatids at the restrictive temperature (30°C), causing chromatin to lag over the spindle midzone[9] (Supplementary Information, Fig. S1). Top2 inactivation did not damage the spindle; at 30°C, localization of the midzone reporters Ase1–GFP and Ipl1–3GFP to anaphase spindles was similar in wild-type and *top2-4* mutant cells (Fig. 1a), which showed no increase in broken spindles. Using the pleckstrin homology domain of phospholipase C fused to GFP (PH–GFP) to visualize the plasma membrane, we next tested whether lagging chromatin affected cytokinesis progression. We inspected the plasma membrane at the bud neck of anaphase and telophase cells, that is, with one spindle-pole body (SPB, visualized using Spc42–CFP as a reporter) in the bud, and scored whether neck membranes were open, contracted or resolved into two separate membranes (Fig. 1b). The fraction of cells with an open bud neck was comparable between *top2-4* (39 ± 5%, mean ± s.d.) and wild-type cells (39 ±2 %), indicating that the onset of furrowing was not delayed. In contrast, the pre-abscission index (the ratio of cells with contracted versus resolved plasma membrane) was increased almost fourfold in the *top2-4* mutant cells, compared with wild-type cells (Fig. 1c, $P < 0.005$), but not in the *top2-4 boi1Δ boi2Δ* triple-mutant cells (Fig. 1c). Thus, cells with defective Top2 form normal spindles yet trigger NoCut and delay abscission.

To test whether lagging chromatin on its own triggers NoCut, we next examined whether failure to separate chromosome arms also affected cytokinesis. Expression of non-cleavable cohesin Scc1[RRDD] blocks nuclear division in the first cycle after release from G_1 phase[10], yet these cells assemble a robust spindle midzone, as shown by the accumulation of Ase1–GFP and Ipl1–3GFP (Fig. 1d). These cells failed to complete septation and separate from their buds, and became bi-budded (Fig. 1e). These bi-budded cells were not resolved on cell wall digestion by zymolyase (Fig. 1f, $P < 0.001$, compared with the wild-type). In contrast, most of the *GAL:SCC1[RRDD];boi1Δ;boi2Δ* mutant cells completed cytokinesis similarly to wild-type cells (Fig. 1e, f, $P < 0.002$, compared with *GAL:SCC1[RRDD]*). Unlike the *GAL:SCC1[RRDD]* single mutant, these triple-mutant cells developed a penetrant 'cut' phenotype, with nuclei cleaved
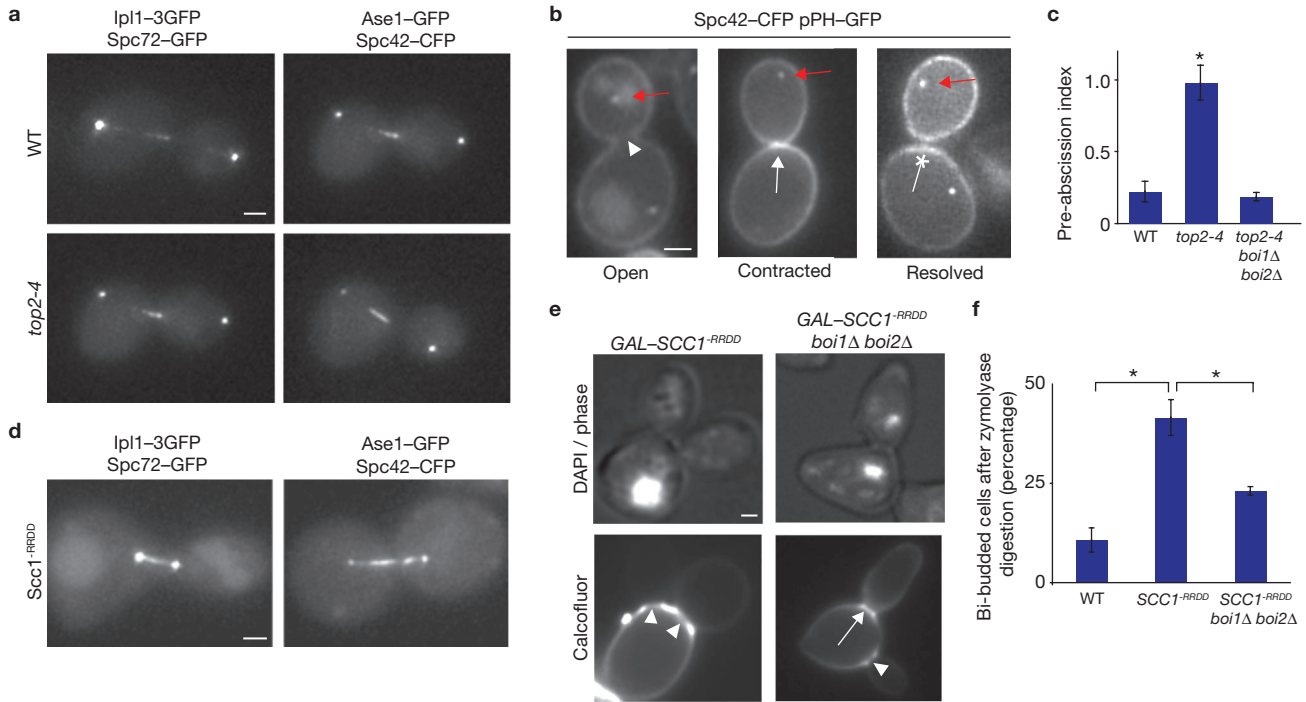
Figure 1 Defects in chromosome segregation trigger NoCut-dependent inhibition of cytokinesis in the absence of midzone damage. (**a**) Localization of the central spindle components Ase1 and Ipl1 in wild-type (WT) and *top2-4* mutants. (**b**) Configuration of the plasma membrane (PH–GFP) in anaphase and post-anaphase cells with one SPB (Spc42–CFP, red arrows) segregated into the bud. White symbols indicate open (arrowhead), contracted (arrow) or resolved (asterisk) bud neck membranes. (**c**) Quantification of the pre-abscission index (fraction of cells with contracted/resolved membranes) in cells of the indicated strains. Except when indicated otherwise, in this and following graphs statistically significant differences (*P* < 0.02) are highlighted with an asterisk. Data are mean ± s.d., *n* = 3 (**d**) Localization of Ase1 and Ipl1 in cells expressing the non-cleavable cohesin Scc1[RRDD]. (**e**) DAPI/phase and calcofluor white cell wall staining of *BOI1 BOI2* and *boi1 boi2* cells expressing Scc1[RRDD] under the control of the *GAL* promoter (*GAL–SCC1[RRDD]*). Arrowheads point to open bud necks and the arrow points to a completed septum. (**f**) Fraction of bi-budded cells in the indicated strains after septum digestion with zymolyase. In **a**–**c**, WT and *top2-4* cells were grown at 30 °C for 4 h. Strains expressing Scc1[RRDD] and cells in **d**–**f** were released from a G$_1$ arrest in galactose medium at 37 °C and examined after 90 min (**d**) or 4 h (**e**, **f**). Scale bars, 1 μm.

into unequal masses (Fig. 1e). Thus, in the absence of midzone damage, cells unable to separate chromosome arms during anaphase triggered NoCut and cytokinesis was aborted.

Non-cleavable cohesin impaired cytokinesis, but preventing chromosome separation by inactivating separase/Esp1 did not. Four hours after release from G$_1$ at the restrictive temperature (37 °C), the *esp1-1* cells became bi-budded. However, cell wall digestion efficiently resolved these aggregates, showing that cytokinesis was complete (Fig. 2a). Accordingly, calcofluor staining established that they had completed septation (Fig. 2b). Because the *esp1-1* mutant is defective in chromosome segregation but not in cytokinesis, cell division should lead to DNA damage in this mutant. Indeed, foci of the DNA damage reporter protein Ddc1–GFP[11] accumulated in *esp1-1* cells during the late stages of division (Fig. 2c). Preventing cytokinesis using the *cdc12-6* septin mutation suppressed the accumulation of such damage (*esp1-1;cdc12-6*, Fig. 2c). Thus, separase inactivation led to a cut phenotype; cytokinesis proceeded in the absence of chromosome segregation and damaged DNA.

Together, these results suggest that Esp1 contributed to the coordination of cytokinesis with chromosome segregation. On release from G$_1$ arrest at the restrictive temperature (37 °C), *ndc10-1* mutant cells prematurely break their spindle and cytokinesis fails, leading to the accumulation of bi-budded cells that are not resolved on cell wall digestion[1] (Fig. 2d, *P* < 0.01, compared with wild-type). In contrast, *ndc10-1;esp1-1* double-mutant cells were effectively resolved into unbudded and single-budded

cells by zymolyase treatment. Furthermore, plasma membrane and cell wall imaging showed that these cells properly completed abscission and septation, unlike the *ndc10-1* single-mutant cells (Fig. 2e). Thus, separase function was required to inhibit abscission in cells with a fragile spindle. We conclude that NoCut function depends on separase.

Early in yeast anaphase, separase cleaves cohesin to resolve sister-chromatid cohesion[12], and promotes activation of the protein phosphatase Cdc14 (ref 13, 14). This latter function is independent of the proteolytic activity of separase; protease-dead Esp1[C1531A] successfully mediates Cdc14 activation, but not cohesin cleavage[15]. Remarkably, expression of Esp1[C1531A] impaired cytokinesis *in esp1-1* single- and *ndc10-1 esp1-1* double-mutant cells, as shown by calcofluor staining and zymolyase digestion (Fig. 3a, b). In contrast, Esp1[C1531A] expression did not impair cytokinesis in wild-type cells. Thus, the non-catalytic function of separase is required for cytokinesis inhibition in response to both spindle and chromosome segregation defects.

In addition to separase, the FEAR network, including the nucleolar proteins Bns1 and Spo12, and the spindle-associated factor Slk19, is also required for Cdc14 activation in early anaphase[14]. Zymolyase digestion and imaging of the septum and plasma membrane (Fig. 3c, d) showed that, in contrast to the *ndc10-1* single-mutant, the *ndc10-1;bns1Δ;spo12Δ* triple-mutant completed cytokinesis efficiently within 4 h. Inactivation of Slk19 in the *ndc10-1* background also restored membrane resolution and septation (Fig. 3d). Deletion of *BNS1* and *SPO12* or *SLK19* did
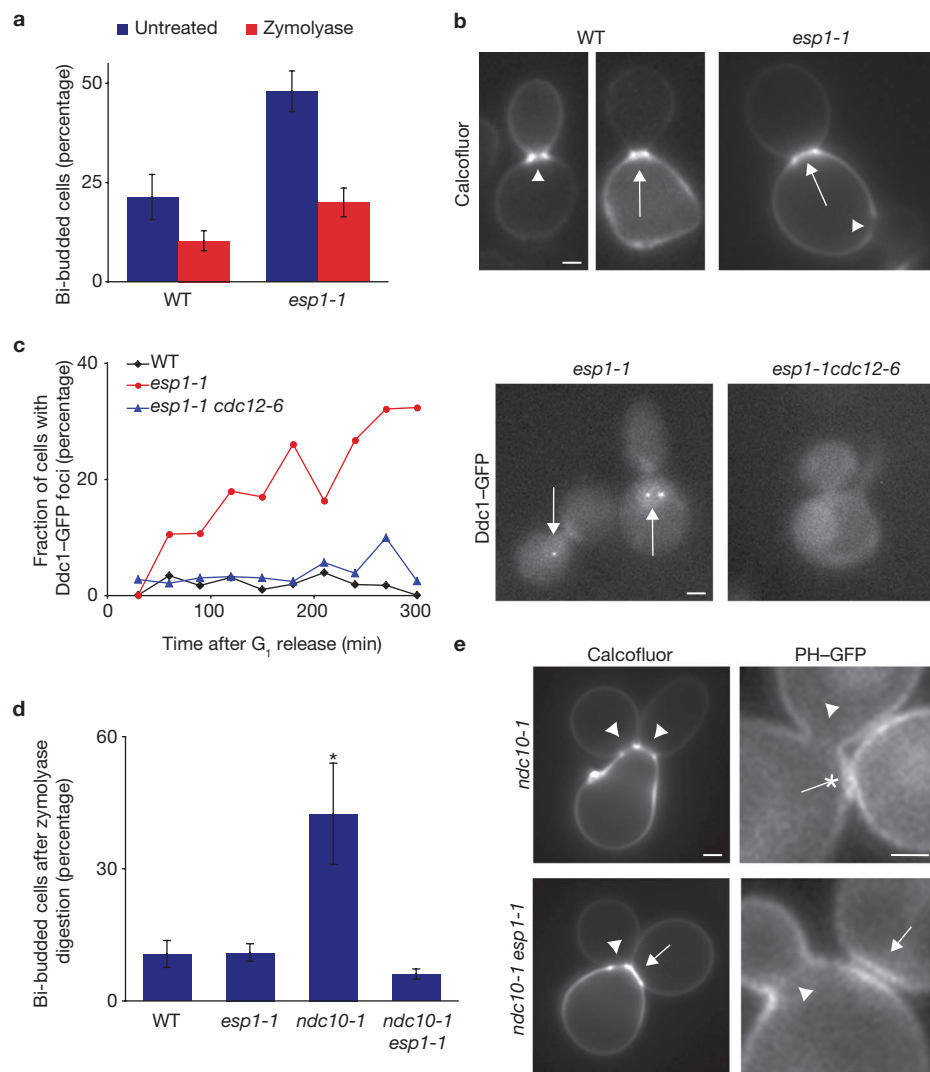
Figure 2 Separase is required for the NoCut response. (**a**) Wild-type (WT) and *esp1-1* cells were released from G₁ arrest at 37°C for 4 h and the fraction of multi-budded cells was determined before and after digestion of the cell wall with zymolyase. Data are mean ± s.d., $n = 3$. (**b**) Calcofluor white staining of the cell wall and septum in WT and *esp1-1* mutant cells. Open bud necks are marked with arrowheads and arrows point to completed septa. (**c**) Time-course of Ddc1–GFP foci formation (left panel). Data shown are from one representative experiment. Nuclear foci of Ddc1–GFP (arrows), corresponding to DNA double-strand breaks, were observed in *esp1-1* cells but not in *esp1-1 cdc12-6* cells (right panel). (**d**) Fraction of bi-budded cells in the indicated strains following septum digestion with zymolyase. Data are mean ± s.d., $n = 3$. (**e**) Status of the division septum (stained with calcofluor) and plasma membrane (PH–GFP) in cells of the indicated strains. Arrowheads point to open septa or open bud neck membranes; arrows point to complete septa or resolved membranes; asterisks mark contracted membranes. Cells of the indicated strains were arrested in G₁ with α-factor, released in fresh medium at 37°C and analysed every 30 min (**c**) or after 4 h. Scale bars, 1 μm.

not suppress the spindle fragility of the *ndc10-1* cells (Supplementary Information, Fig. S2). Similarly, *bns1Δ spo12Δ* mutant cells expressing Scc1^RRDD underwent two rounds of budding within 4 h without cytokinesis failure, and did not accumulate as zymolyase-resistant bi-budded cells (Fig. 3c). Thus, the NoCut response to fragile spindles and sister chromatid resolution defects depended on FEAR function.

Because Cdc14 mediates both mitotic exit and cytokinesis onset[16], we could not directly test whether it has a role in inhibiting cytokinesis completion. Instead, we assessed whether dephosphorylation of a known Cdc14 target contributes to NoCut function. Interestingly, Cdc14 regulates the CPC by dephosphorylating INCENP/Sli15 at the onset of anaphase. Sli15 dephosphorylation depends on FEAR and targets CPC to the central spindle[17]. To investigate whether NoCut function requires Sli15

dephosphorylation, we tested whether constitutively dephosphorylated Sli15, Sli15-6A[18], could restore NoCut in FEAR-defective cells. In contrast to *esp1-1* and *ndc10-1 esp1-1* mutant cells, cell wall digestion and imaging of septa and plasma membrane all indicated that cytokinesis was aborted in many *esp1-1 SLI15-6A* ($P < 0.01$, compared with *esp1-1*) and *ndc10-1 esp1-1 SLI15-6A* ($P < 0.0001$, compared with *ndc10-1 esp1-1*) mutant cells (Fig. 3e, f). Thus, non-phosphorylatable Sli15 restored NoCut function in FEAR defective cells. It also restored Ipl1–3GFP recruitment to the spindle in the *esp1-1* and *ndc10-1 esp1-1* cells, as predicted[17] (Fig. 3g and data not shown), as well as Ase1 localization in *ndc10-1 esp1-1* mutant cells (Fig. 3i). Thus, Cdc14-dependent regulation of CPC accounted for most, if not all, FEAR requirement in NoCut. Importantly, expression of Sli15-6A caused cytokinesis to be aborted only in the *esp1-1* and *ndc10-1*
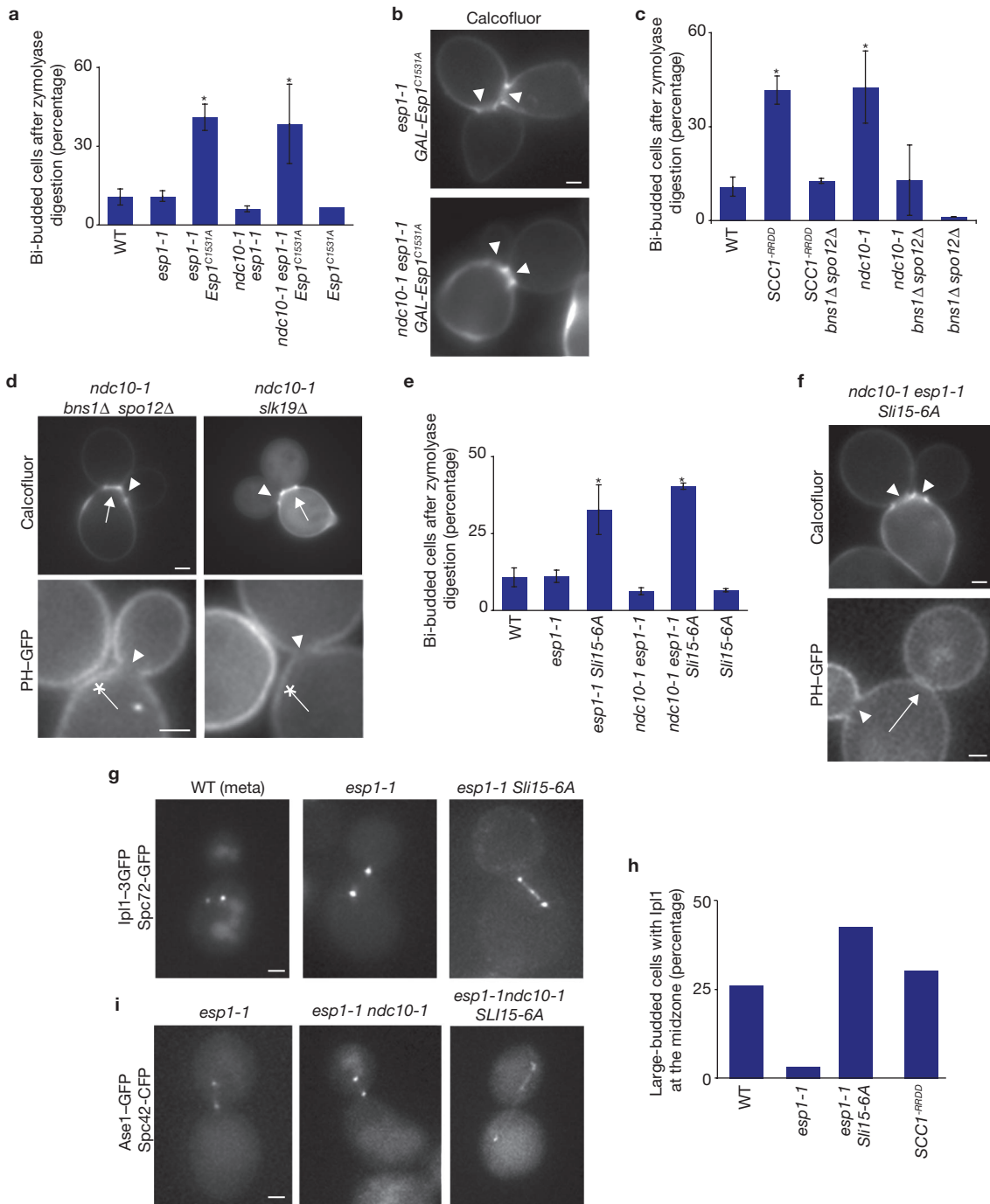
Figure 3 FEAR is required for the NoCut response through Ipl1 targeting to spindle microtubules. (**a**, **c**, **e**) Fraction of bi-budded cells after septum digestion with zymolyase. (**b**, **d**, **f**) Status of the division septum (stained with calcofluor) and of the plasma membrane (PH–GFP) in cells of the indicated strains. Arrowheads point to open septa or open bud neck membranes and arrows point to complete septa and contracted membranes; asterisks mark resolved membranes. (**g**–**i**) Recruitment of Ipl1–3GFP and Ase1–GFP to the spindle midzone in large-budded cells of the indicated strains after 2 h at 37°C. A small-budded, metaphase wild-type cell is shown in **g** for comparison; $SCC1^{RRDD}$ midzones are shown in Fig. 1d. In all panels, cells were arrested in G_1 with α-factor and then released in fresh galactose (for $Scc1^{RRDD}$ and $Esp1^{C1531A}$ induction) or glucose medium at 37°C for 4 h before processing. Scale bars, 1 μm.

esp1-1 cells, but not in the wild-type. Therefore, recruitment of CPC to the midzone is required for NoCut to sense spindle and sister chromatid resolution defects, but does not trigger NoCut on its own.

Independently, while screening for NoCut genes (H.R. and Y.B., unpublished observations) we identified chromatin components, including Ahc1,

a scaffolding element of the ADA histone acetyltransferase[19]. In support of Ahc1 functioning in NoCut, *ndc10-1 ahc1Δ* cells failed to inhibit abscission, as shown by the reduction in the number of multi-budded cells following zymolyase treatment (Fig. 4a). Further, the double mutant *ahc1Δ ase1Δ* showed reduced viability when compared with either single mutant
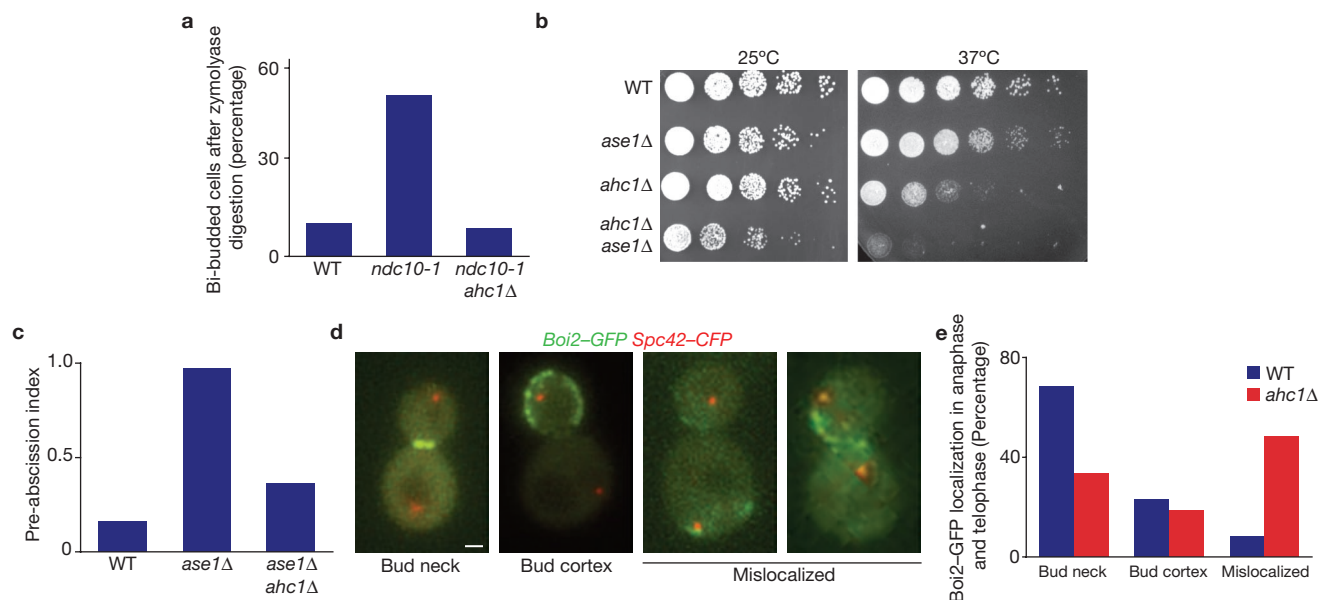
Figure 4 The ADA histone acetyltransferase component Ahc1 is required for the NoCut response. (**a**) Fraction of bi-budded cells following septum digestion with zymolyase. Cells were released from G$_1$ arrest at 37°C for 4 h before processing. (**b**) Threefold serial dilutions of cells of the indicated strains were plated on YPD and grown for 2–3 days at the indicated temperatures. (**c**) Quantification of the pre-abscission index (fraction of cells with contracted/resolved membranes) in cells of the indicated strains expressing Spc42–CFP and PH–GFP. (**d**, **e**) Localization of Boi2–GFP (green) in wild-type (WT) and *ahc1Δ* cells expressing Spc42–CFP (red). In **c**–**e**, cells were grown in minimal medium at 23°C. Scale bars, 1 μm.

(Fig. 4b). Because *ase1Δ* cells rely on NoCut to prevent chromosome damage[1], this observation suggests that Ahc1 is required to delay abscission in cells with anaphase-spindle defects. Accordingly, although the pre-abscission index of *ase1Δ* cells was increased as reported[1], this abscission delay was suppressed in the *ahc1Δ ase1Δ* cells (Fig. 4c). Furthermore, localization of the NoCut effector Boi2 to the cleavage site was perturbed in *ahc1Δ* mutant cells (Fig. 4d, e). Therefore, the chromatin component Ahc1 was required for proper NoCut function in cells with anaphase defects.

These observations raise the possibility that chromatin is directly involved in NoCut sensing. As chromatin is a potent activator of Aurora B *in vitro*[20], the CPC on the midzone may signal the presence of chromatin. We rationalized that if this is correct, preventing CPC segregation away from chromatin should trigger NoCut independently of chromosome segregation defects or spindle damage. To test this possibility, Ipl1 was fused to the Tet repressor and YFP (Ipl1–TetR–YFP) to tether it to chromatin in cells carrying Tet operator (*TetO*) repeats. Expression of Ipl1–TetR–YFP did not affect growth of wild-type cells and fully complemented the *ipl1-321* mutant (Fig. 5a). Furthermore, like wild-type Ipl1, the fusion protein localized to two dots located between the two spindle poles of metaphase cells, probably the kinetochores, and to the spindle midzone during anaphase (Fig. 5b). In cells containing *TetO* repeats, one or two supplementary YFP foci were observed in metaphase and anaphase nuclei, respectively (Fig. 5c). Thus, a fraction of Ipl1–TetR–YFP successfully attached to chromatin in these cells.

We determined the pre-abscission index of cells co-expressing Ipl1–TetR–YFP, Spc42–CFP and PH–GFP, and containing TetO arrays on the sub-telomeric region of chromosome XII (*tetO:TEL12R*) or near the centromere of chromosome IV (*tetO:TRP1*). The fraction of cells with an open bud neck was comparable in *TetO:TEL12R* cells carrying an empty plasmid or expressing Ipl1–TetR–YFP (control, 41.5 ± 6.1%; Ipl1–TetR–YFP, 37.8 ± 6.3%). In contrast, the pre-abscission index was increased 2.5-fold in *IPL1–TetO:TEL12R* cells expressing the Ipl1–TetR–YFP

fusion, compared with *TetO* cells carrying an empty plasmid (Fig. 5d, *P* < 0.005;). This increase was independent of the position of the TetO array on the chromosome, as Ipl1–TetR elicited a comparable effect in *tetO:TRP1* and *tetO:TEL12R* (Supplementary Information, Fig. S3). As these effects were observed in the presence of wild-type, endogenous Ipl1, the Ipl1–TetR construct acted dominantly.

The inhibition of abscission caused by Ipl1–TetR required Ipl1 kinase activity; TetR fused to kinase-dead Ipl1 (Ipl1^{D227A})[21] did not delay abscission. Furthermore, Ipl1–TetR did not inhibit abscission of *IPL1;boi1Δ;boi2Δ;tetO:TEL12R* cells (Fig. 5e). Thus, Ipl1 tethering to chromatin led to a NoCut-dependent abscission delay. This delay was not due to spindle stabilization or destabilization by Ipl1–TetR, as the fraction of cells undergoing anaphase was not altered by Ipl1–TetR expression (Supplementary Information, Fig. S4). Furthermore, Ipl1–TetR–YFP fully bypassed the requirement for FEAR and ADA function in NoCut activation; Ipl1–TetR–YFP sucessfully activated NoCut in *slk19Δ* TetO and *ahc1Δ* TetO cells (Fig. 5e). Thus, although simultaneous occurrence of Ipl1 on the spindle midzone and lagging chromatin around it is normally required to trigger NoCut, these requirements were bypassed when Ipl1 was forced onto chromatin. In addition, these results indicate that Ahc1 contributes to NoCut upstream of Ipl1 function. Clustering of aurora-B can lead to its activation, as observed when two CPC complexes are brought together with specific antibodies[20]. However, the effect of 'clustering-mediated' activation of Ipl1 is probably limited, as TetR-mediated dimerization[22] caused only a mild abscission delay on its own, that is, in cells lacking TetO sequences (Fig. 5d, *P* < 0.008). We conclude that tethering Ipl1 to chromatin mimics the events required for the activation of the NoCut response in cells with chromosome segregation and spindle defects.

In summary, our data show that 1) NoCut is triggered by the presence of unsegregated chromatin lagging over the spindle midzone, even in the absence of spindle defects; 2) NoCut function requires targeting of the CPC
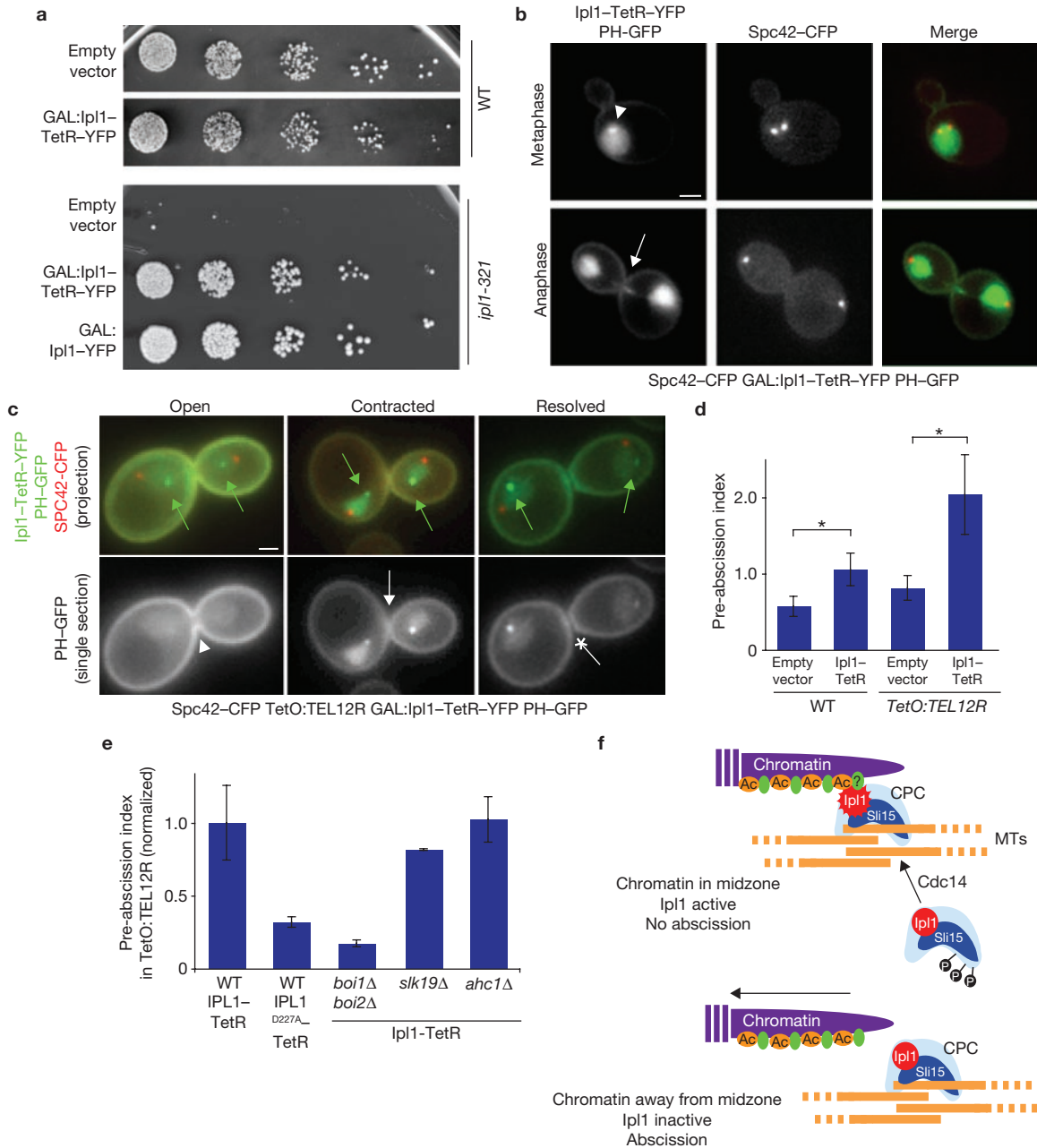
481

Figure 5 Tethering of Ipl1 to chromosome arms triggers the NoCut response. (**a**) Threefold serial dilutions of wild-type (WT) or *ipl1-321* cells bearing control, Ipl1–YFP- or Ipl1–TetR–YFP-encoding plasmids were plated on galactose medium and grown for 3 days at 35°C. (**b**, **c**) Localization of Ipl1–TetR–YFP (green) and Spc42–CFP (red) in wild-type (**b**) or *TetO* strains expressing the membrane marker PH–GFP (green; **c**). Arrowhead, nuclear focus possibly corresponding to kinetochores in the metaphase cell; arrow, spindle midzone in the anaphase cell (**b**). Green arrows, Ipl1 foci at chromosomal *TetO:TEL12R* arrays in anaphase and telophase cells; white symbols indicate open (arrowhead), contracted (arrow) or resolved (asterisk) bud neck membranes (**c**). Scale bars, 1 μm. (**d**, **e**) Pre-abscission index (fraction of cells with contracted/resolved membranes) in cells of the indicated strains expressing Ipl1–TetR fusions. (**f**) A model for how Aurora monitors chromatin segregation during anaphase. Upper panel: in early anaphase, separase and FEAR-dependent activation of Cdc14 targets the CPC (the Ipl1 and Sli15 subunits are depicted in red and blue, respectively) to spindle midzone microtubules (MTs; in orange). We speculate that Ipl1 is activated there through interaction with chromatin-associated factors (in green; chromosomes are depicted in purple), which require Ahc1 function to interact with midzone-bound CPC. As a result, abscission is inhibited. Lower panel: on completion of chromosome segregation, the CPC is no longer activated by chromatin and the NoCut signal is turned off, thus abscission ensues.

to the central spindle during anaphase, indicating that the NoCut signal is generated at this location and time; 3) The chromatin component Ahc1 contributes upstream of Ipl1 to proper NoCut activation. As Ahc1 is a core component of the histone acetylation complex ADA, acetylation events might trigger or be required for Ipl1 to detect anaphase defects. Remarkably,

ahc1Δ mutant cells not only failed to inhibit abscission in response to anaphase defects, but also showed a high incidence of DNA damage[23]. At least some of this damage may result from NoCut inactivation[1]. 4) Holding Ipl1 in contact with chromatin throughout anaphase triggers the NoCut response independently of anaphase defects, Ahc1 function, FEAR and

proper localization of Ipl1 to the spindle midzone. Together, these data suggest that the CPC acts as a sensor that activates NoCut in response to the presence of chromatin around the spindle midzone (Fig. 5f). This model explains why abscission is delayed in response to situations as distinct as the presence of chromosome bridges and premature spindle breakage.

Studies in *Schizosaccharomyces pombe* identified the *cut* mutants, which block anaphase yet proceed through cytokinesis, cutting the undivided nucleus[24]. These findings suggest that cytokinesis is not coordinated with chromosome segregation in eukaryotes. However, the cut phenotype may be attributed to NoCut delaying rather than preventing cytokinesis, as we observed in the *top2-4* mutant. Indeed, these cells do eventually complete cytokinesis, which causes DNA damage[25] and cell death. Alternatively, *cut* mutants may impair both chromosome segregation and NoCut. Indeed, the *S.cerevisiae* separase mutant *esp1-1* also develops a cut phenotype, but as we show, this is because separase is required for mounting the NoCut response. Thus, NoCut seems to be conserved in evolution. The *cut* gene collection will probably provide an excellent resource for further dissection of the NoCut checkpoint. □

METHODS

Strains and plasmids. All yeast strains are derivatives of S288C. *SPC72–GFP* and *ASE1–GFP* strains have been described previously[26]. Gene deletion strains were obtained from EUROSCARF[27] or were generated by PCR-based gene disruption. The Boi2–GFP plasmid has been described previously[1]. *tetO* strains were gifts from Luis Aragón (MRC, London) and Duncan Clarke (University of Minnesota, Minneapolis, MN). Ipl1 constructs were cloned into pRS416 (ref. 28) and the kinase dead *Ipl1* allele was generated by site-directed mutagenesis (QuickChange, Stratagene). The pleckstrin homology domain of *Rattus norvegicus* phospholipase C ∂1 fused to GFP (PH–GFP), a gift from Scott Emr (Howard Hughes Medical Institute, Bethesda, MD), was expressed from pRS426-based plasmids[29]. The *Sli15-6A* allele is identical to that described previously[17] except in the choice of one phosphorylation site: Ser 335, 427, 437, 448, 462 and Thr 474 were mutated to Ala.

Growth conditions and staining procedures. Cells were grown in rich medium (YPD) at room temperature, unless indicated otherwise. For synchronization experiments, cells were arrested with α-factor (10 µg ml⁻¹; Sigma) for 2–4 h at 22°C, washed twice in fresh medium and released at the restrictive temperature (for temperature-sensitive mutants) or at 22°C. For galactose induction, cells were arrested with α-factor in YP + 2% raffinose, released in YP + raffinose + 2% galactose and examined after 4–5 h. Expression of Ipl1 constructs was induced by addition of galactose (2%) to exponentially growing cultures in selective raffinose medium at 22°C. Cells were examined 4–5 h after galactose addition (8 h for *ahc1Δ*). For DAPI staining, cells were fixed for 30 min in 70% ethanol, washed in PBS and resuspended in PBS containing 1 µg ml⁻¹ DAPI. For calcofluor staining and septum digestion, cells were fixed with 3.7% formaldehyde for 30 min and washed twice with PBS. Calcofluor (Sigma) was used at 0.01 mg ml⁻¹ in PBS.

Microscopy. Imaging was performed on Olympus BX50 and Leica AF7000 fluorescence microscopy systems equipped with a piezo motor, as described previously[30]. Spindle images are maximum projections of *z*-stacks; plasma membrane status was evaluated on single, non-confocal *z* axis slices (9 stacks spaced 300 nm).

Cytokinesis assays. The frequency of multi-budded (cytokinesis-defective) cells was evaluated by light microscopy after 30 min digestion with zymolyase (2 mg ml⁻¹) in 1 M sorbitol at 22°C. Pre-abscission indices of cells expressing PH–GFP and Spc42–CFP were calculated as (fraction of cells with contracted bud neck membranes)/(fraction of cells with resolved membranes). Only cells in which one SPB had entered the bud were considered for analysis. In all cases, the fraction of cells with open bud necks did not change significantly (*P* > 0.05). Results of abscission and zymolyase assays are expressed as the mean ± s.d. of at least three independent experiments. More than 100 cells were counted for each condition.

Statistical analysis. Unpaired two-tailed *t*-tests allowing for unequal variance were used (Microsoft Excel).

1. Norden, C. *et al*. The NoCut pathway links completion of cytokinesis to spindle midzone function to prevent chromosome breakage. *Cell* 125, 85–98 (2006).
2. Steigemann, P. *et al*. Aurora B-mediated abscission checkpoint protects against tetraploidization. *Cell* 136, 473–484 (2009).
3. Musacchio, A. & Salmon, E. D. The spindle-assembly checkpoint in space and time. *Nature Rev. Mol. Cell Biol.* 8, 379–393 (2007).
4. May, K. M. & Hardwick, K. G. The spindle checkpoint. *J. Cell Sci.* 119, 4139–4142 (2006).
5. Barr, F. A. & Gruneberg, U. Cytokinesis: placing and making the final cut. *Cell* 131, 847–860 (2007).
6. Eggert, U. S., Mitchison, T. J. & Field, C. M. Animal cytokinesis: from parts list to mechanisms. *Annu. Rev. Biochem.* 75, 543–566 (2006).
7. Ruchaud, S., Carmena, M. & Earnshaw, W. C. Chromosomal passengers: conducting cell division. *Nature Rev. Mol. Cell Biol.* 8, 798–812 (2007).
8. Vader, G., Medema, R. H. & Lens, S. M. The chromosomal passenger complex: guiding Aurora-B through mitosis. *J. Cell Biol.* 173, 833–837 (2006).
9. Holm, C., Goto, T., Wang, J. C. & Botstein, D. DNA topoisomerase II is required at the time of mitosis in yeast. *Cell* 41, 553–563 (1985).
10. Uhlmann, F., Lottspeich, F. & Nasmyth, K. Sister-chromatid separation at anaphase onset is promoted by cleavage of the cohesin subunit Scc1. *Nature* 400, 37–42 (1999).
11. Melo, J. A., Cohen, J. & Toczyski, D. P. Two checkpoint complexes are independently recruited to sites of DNA damage *in vivo*. *Genes Dev.* 15, 2809–2821 (2001).
12. Uhlmann, F., Wernic, D., Poupart, M. A., Koonin, E. V. & Nasmyth, K. Cleavage of cohesin by the CD clan protease separin triggers anaphase in yeast. *Cell* 103, 375–386 (2000).
13. Queralt, E., Lehane, C., Novak, B. & Uhlmann, F. Downregulation of PP2A(Cdc55) phosphatase by separase initiates mitotic exit in budding yeast. *Cell* 125, 719–732 (2006).
14. Stegmeier, F., Visintin, R. & Amon, A. Separase, polo kinase, the kinetochore protein Slk19, and Spo12 function in a network that controls Cdc14 localization during early anaphase. *Cell* 108, 207–220 (2002).
15. Sullivan, M. & Uhlmann, F. A non-proteolytic function of separase links the onset of anaphase to mitotic exit. *Nature Cell Biol.* 5, 249–254 (2003).
16. Stegmeier, F. & Amon, A. Closing mitosis: the functions of the Cdc14 phosphatase and its regulation. *Annu. Rev. Genet.* 38, 203–232 (2004).
17. Pereira, G. & Schiebel, E. Separase regulates INCENP-Aurora B anaphase spindle function through Cdc14. *Science* 302, 2120–2124 (2003).
18. Higuchi, T. & Uhlmann, F. Stabilization of microtubule dynamics at anaphase onset promotes chromosome segregation. *Nature* 433, 171–176 (2005).
19. Eberharter, A. *et al*. The ADA complex is a distinct histone acetyltransferase complex in *Saccharomyces cerevisiae*. *Mol. Cell. Biol.* 19, 6621–6631 (1999).
20. Kelly, A. E. *et al*. Chromosomal enrichment and activation of the aurora B pathway are coupled to spatially regulate spindle assembly. *Dev. Cell* 12, 31–43 (2007).
21. King, E. M., Rachidi, N., Morrice, N., Hardwick, K. G. & Stark, M. J. Ipl1p-dependent phosphorylation of Mad3p is required for the spindle checkpoint response to lack of tension at kinetochores. *Genes Dev.* 21, 1163–1168 (2007).
22. Ramos, J. L. *et al*. The TetR family of transcriptional repressors. *Microbiol Mol. Biol. Rev.* 69, 326–356 (2005).
23. Alvaro, D., Lisby, M. & Rothstein, R. Genome-wide analysis of Rad52 foci reveals diverse mechanisms impacting recombination. *PLoS Genet.* 3, e228 (2007).
24. Yanagida, M. Fission yeast cut mutations revisited: control of anaphase. *Trends Cell Biol.* 8, 144–149 (1998).
25. Baxter, J. & Diffley, J. F. Topoisomerase II inactivation prevents the completion of DNA replication in budding yeast. *Mol. Cell* 30, 790–802 (2008).
26. Huh, W. K. *et al*. Global analysis of protein localization in budding yeast. *Nature* 425, 686–691 (2003).
27. Winzeler, E. A. *et al*. Functional characterization of the *S. cerevisiae* genome by gene deletion and parallel analysis. *Science* 285, 901–906 (1999).
28. Sikorski, R. S. & Hieter, P. A system of shuttle vectors and yeast host strains designed for efficient manipulation of DNA in *Saccharomyces cerevisiae*. *Genetics* 122, 19–27 (1989).
29. Christianson, T. W., Sikorski, R. S., Dante, M., Shero, J. H. & Hieter, P. Multifunctional yeast high-copy-number shuttle vectors. *Gene* 110, 119–122 (1992).
30. Kusch, J., Meyer, A., Snyder, M. P. & Barral, Y. Microtubule capture by the cleavage apparatus is required for proper spindle positioning in yeast. *Genes Dev.* 16, 1627–1639 (2002).

483

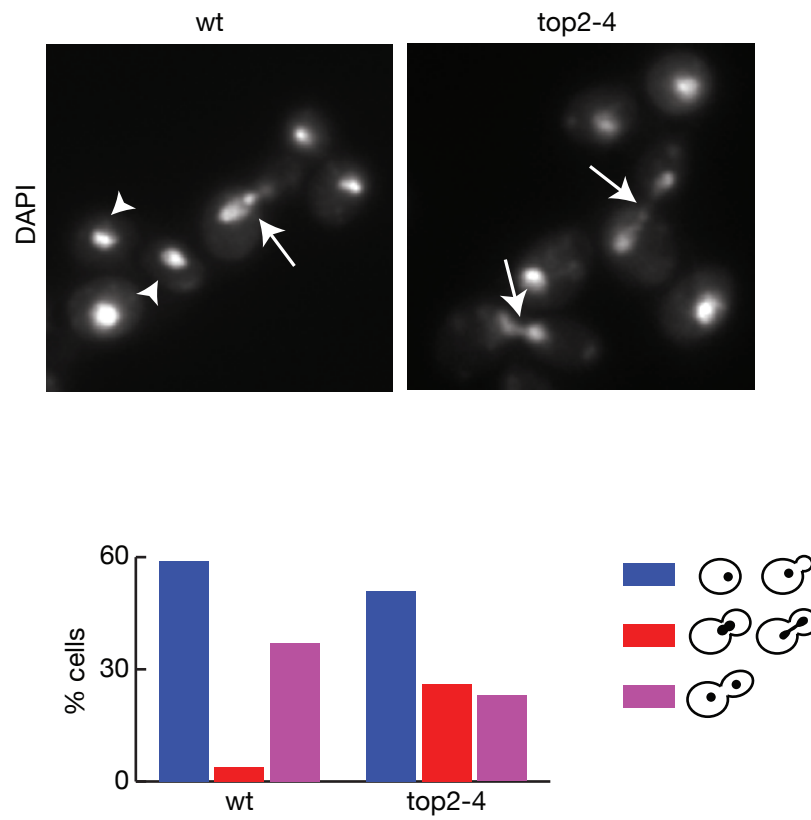**nature**
cell biology

Figure S1 *top2-4* mutants incompletely segregate their chromosomes, visualized by DAPI. Arrowheads point at post-anaphase nuclei; arrows point at elongated anaphase nuclei in wild type (left) and to chromosome bridges in *top2-4* mutant cells. Cells (N>100) were grown at 30°C for 4 hours.
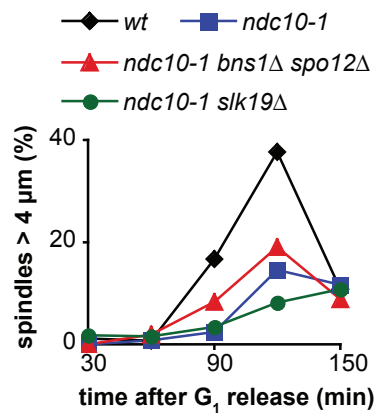
Figure S2 Quantification of spindle elongation, as determined by the distance between SPBs, in Spc42-CFP expressing cells of the indicated strains. Cells were arrested in G_1 with alpha-factor, released in fresh media at 37°C, and analyzed every 30 min.

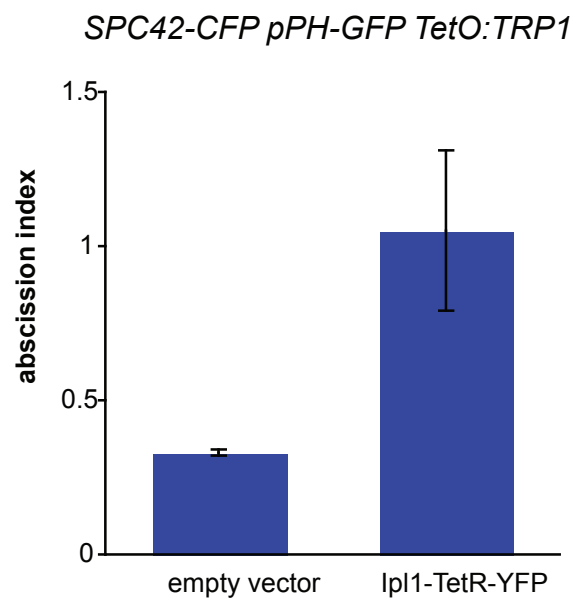## SPC42-CFP pPH-GFP TetO:TRP1

Figure S3 Pre-abscission index (fraction of cells with contracted / resolved membranes) in *tetO:TRP1* cells expressing Ipl1-TetR-YFP. Expression was induced in galactose media for 4 hours.
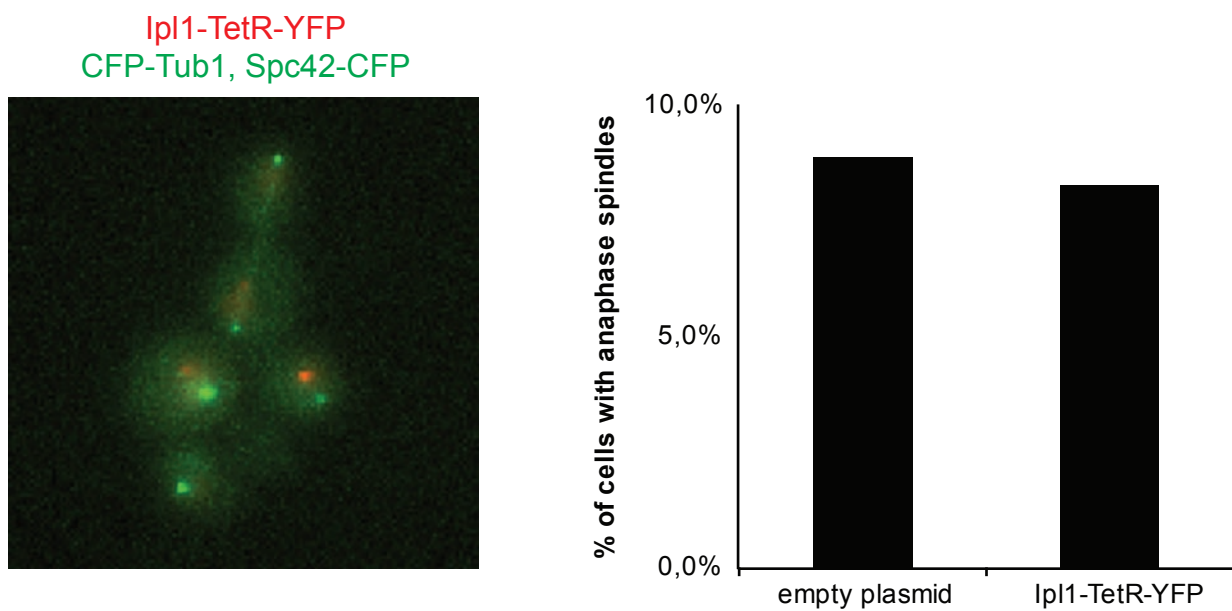
Figure S4 Ipl1-TetR-YFP does not delay spindle disassembly. The fraction of cells with elongated spindles (green arrow) was quantified in a *TetO:TEL12R CFP-TUB1 SPC42-CFP* strain bearing either a control or Ipl1-TetR-YFP encoding plasmid. Cells were grown in galactose media for 4 hours to induce Ipl1-TetR-YFP expression (red arrows). N > 300.